Mon. Not. R. Astron. Soc. **398,** 1512–1526 (2009) doi:10.1111/j.1365-2966.2009.15220.x

An analysis of the region of the Phocaea dynamical family

V. Carruba[1,2]★

[1]*IPD, UNIVAP, São José dos Campos, SP, 12244-000, Brazil*
[2]*Department of Mathematics, UNESP, Guaratinguetá, SP, Brazil*

Accepted 2009 June 9. Received 2009 June 9; in original form 2009 March 10

ABSTRACT

In this work, I conduct a preliminary analysis of the Phocaea family region. I obtain families and clumps in the space of proper elements and proper frequencies, study the taxonomy of the asteroids for which this information is available, analyse the albedo and absolute magnitude distribution of objects in the area, obtain a preliminary estimate of the possible family age, study the cumulative size distribution and collision probabilities of asteroids in the region, the rotation rate distribution and obtain dynamical map of averaged elements and Lyapunov times for grids of objects in the area.

Among my results, I identified the first clump visible only in the frequency domain, the (6246) Komurotoru clump, obtained a higher limit for the possible age of the Phocaea family of 2.2 Byr, identified a class of Phocaea members on Mars-crossing orbits characterized by high Lyapunov times and showed that an apparently stable region on time-scales of 20 Myr near the ν_6 secular resonance is chaotic, possibly because of the overlapping of secular resonances in the region. The Phocaea dynamical group seems to be a real S-type collisional family, formed up to 2.2 Byr ago, whose members with a large semimajor axis have been dynamically eroded by the interaction with the local web of mean-motion and secular resonances. Studying the long-term stability of orbits in the chaotic regions and the stability of family and clumps identified in this work remain challenges for future works.

Key words: celestial mechanics – minor planets, asteroids.

1 INTRODUCTION

Among highly inclined asteroids [asteroids with $\sin(i) > 0.3$, for which the analytical theory used to obtain proper elements is not very accurate (Milani & Knežević (1994)], the asteroids in the region of the Phocaea family are characterized by a very interesting dynamics. The region of the Phocaea family is delimited by the 7J:-2A mean-motion resonance at low a, by the 3J:-1A resonance at high a and by the $\nu_6 = g - g_6$ (where g is the secular frequency of precession of the pericentre, and the suffix 6 refers to Saturn) secular resonance at low i (Knežević & Milani 2003). A region of shallow close encounters with Mars appears at $e > 0.3$, but deep close encounters with Mars are made impossible by the Kozai-class protection mechanism (Milani et al. 1989). The Phocaea family itself is characterized by its interaction with the $\nu_6 - \nu_{16}$ secular resonance [$(g - g_6) - (s - s_6)$, where s is the secular precession frequency of the asteroid node], and harmonics of this resonance are also present in the region. To better understand the interaction of the Phocaea family with the $(\nu_6 - \nu_{16})$ secular resonance, the family was recently obtained in the (n, g, $g - s$) frequency domain by Carruba & Michtchenko (2009). Other families and clumps in the region were recently identified by Foglia & Masi (2004) and Gil-Hutton (2006).

One of the open questions about the Phocaea family is if the dynamical family is real or an artefact created by the stable island region between secular and mean-motion resonances, and the zone of close encounters with Mars (Knežević & Milani 2003). For the purpose of answering this and other questions in this work, I first re-obtained dynamical families in the space of proper element and frequencies (Carruba & Michtchenko 2007, 2009), I studied the spectroscopical and Sloan Digital Sky Survey Moving Objects Catalogue, fourth release (SDSS-MOC4) data for the region, reviewed the current knowledge on geometric albedos and absolute magnitudes, obtained the Yarkovsky isolines, studied the cumulative distribution and collision probabilities of family members and the information on asteroid rotation rates, and the role that mean-motion and secular resonances have had in shaping the family.

I found that, with the exception of the family around (19536) (1999 JM4), formerly associated with the clump around (2860) Pasacentennium, the families and clumps found by Gil-Hutton (2006) are now substructures of the Phocaea family. I identified new clumps in a proper element and frequency space, and in particular I found the first 'frequency-only' clump around (6246) Komurotoru.

A preliminary analysis of Yarkovsky isolines shows that the family can be up to 2.2 Byr old. Dynamical maps of the region showed

★E-mail: valerio@univap.br

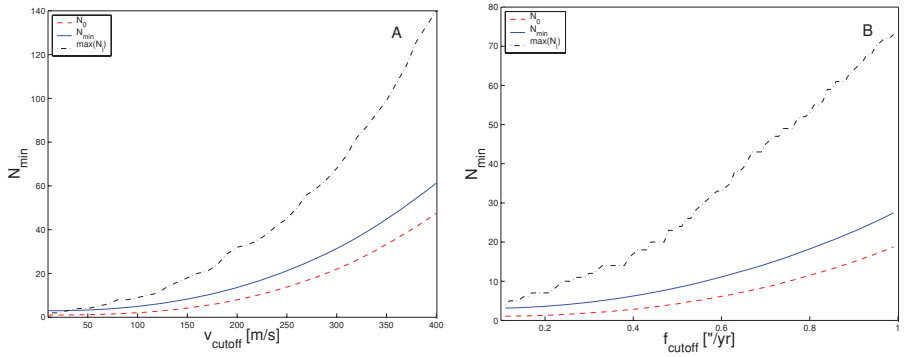

Figure 1. The average number N_0, $N_{\rm min}$ and the maximum number max (N_i) of asteroids as a function of the velocity cut-off (panel A), and of the frequency cut-off (panel B), for the asteroids in the region of the Phocaea family.

us that there exist regions that are dynamically stable on the timescales of the integration, but yet deprived of asteroids. Such regions, all characterized by very low values of Lyapunov times, are either associated with Mars-crossing orbits, or are near the border of the ν_6 secular resonance separatrix. Understanding the long-term stability of orbits in the chaotic regions and the stability of family and clumps identified in this work will be the subject of a next paper on this subject.

2 DYNAMICAL FAMILIES AND CLUMPS IN THE REGION

I start my analysis of the Phocaea family region by re-deriving classical and frequency families and clumps in the area. I identify the members of the dynamical families in the region using the classical hierarchical clustering method [CHCM; see Bendjoya & Zappalà 2002 and references therein], and the frequency hierarchical clustering method (FHCM; Carruba & Michtchenko 2007, 2009).[1]

In identifying asteroid families in the space of proper elements two parameters are fundamental: the cut-off distance at which the family members are defined (d_0) and the minimum number of objects N_{min} for a cluster to be considered significant. Beaugé & Roig (2001) define a nominal distance cut-off as the average minimum distance between all the neighbouring asteroids in the same region of the asteroid belt. The value of $N_{\rm min}$ is defined by Zappalà et al. (1995) as

$$N_{\rm min} = N_0 + 2\sqrt{N_0}, \tag{1}$$

where N_0 is the average number of orbits within a sphere of radius d_0 at every point of the proper element space. A cluster with a number of objects larger than this critical value is called a clump, while a family is a cluster with a number of members larger than $2.5 \times N_{\rm min}$. As we shall see in more detail in Section 8, the region of the Phocaea family is delimited by the 7J:-2A and 3J:-1A mean-motion resonances in proper a and by the ν_6 secular resonance at low inclination. Currently, 1736 objects are found in the AstDyS site in this region. The nominal distance velocity cut-off as defined in Beaugé & Roig (2001) is of 146.9 m s^{-1}, while Fig. 1 displays the average number N_0, $N_{\rm min}$ and the maximum number max (N_i) of asteroids as a function of the velocity cut-off, for asteroids in the region. The value of $N_{\rm min}$ corresponding at $d_0 = 146.9$ m s^{-1} is 8. As can be seen in Fig. 1, the fact that max (N_i) is not much larger than $N_{\rm min}$ may be a hint that the families dominate the local background of objects (see Section 6).

For what concerns the domain of proper frequencies, since the Phocaea group is characterized by its interaction with the $(g - s - g_6 + s_6)$ resonance, or $(\nu_6 - \nu_{16})$ (Knežević & Milani 2003, see also Section 8), following the approach of Carruba & Michtchenko (2009), I determined the family with a metric of the form

$$f = \sqrt{h_1 \left(\frac{\Delta n}{h_0}\right)^2 + h_2(\Delta g)^2 + h_3(\Delta(g-s))^2}, \tag{2}$$

(where $h_1 = h_2 = h_3 = 1$) rather than with the 'standard frequency metric' in the $(n,\ g,\ g + s)$ domain of Carruba & Michtchenko (2007). I determined the nominal frequency cut-off defined as the average minimum distance between all neighbouring asteroids in the $(n,\ g,\ g - s)$ domain, and I found a value of $f_0 = 0.525$ arcsec yr^{-1}. Fig. 1 (panel B) displays the average number N_0, $N_{\rm min}$ and the maximum number max (N_i) of asteroids as a function of the frequency cut-off defined by equation (2). The value of $N_{\rm min}$ corresponding at $f_0 = 0.525$ arcsec yr^{-1} is 26. As observed for the values of $N_{\rm min}$ and max (N_i) obtained in the proper element domain in the domain of frequencies, I still do not observe a much larger value of max N_i with respect to $N_{\rm min}$. Again, this may suggest that the local background of the Phocaea family is indeed dominated by the Phocaea family itself (see Section 6).

Since the Phocaea family is by far the most prominent family in the region, I started by using the CHCM for this family. Fig. 2 (panel A) displays the number of family members (left ordinate) and the differential number dn/dv (right ordinate) as a function of the velocity cut-off. The red vertical line displays the nominal cut-off according to Beaugé & Roig (2001). The numbers on the top of the peaks of differential asteroid numbers are related to the cluster of objects englobed by the Phocaea family. For $d_{\rm cut-off} = 110$ m s^{-1} the Phocaea family conglomerates with the (587) Hypsipyle cluster, at $d_{\rm cut-off} \simeq 130$ the Phocaea families annexed the former Gil-Hutton families associated with (1660) Wood and (5247) Krylov, at $d_{\rm cut-off} = 177$ m s^{-1} the family englobes the newly found family associated with (2860) Pasacentennium [a former clump in Gil-Hutton (2006)] and, finally, at $d_{\rm cut-off} = 198$ m s^{-1} the Phocaea family conglomerates with the last independent clump associated with (17628) 1996 FB5. For higher values of the cut-off, the family simply slowly expands annexing peripheral objects. This may suggest that the local background of the Phocaea family is dominated by the Phocaea family itself. I will come back to this subject in the following sections.

[1] I used synthetic proper elements and frequencies obtained numerically and is publically available at the AstDyS site http://hamilton.dm.unipi.it/cgi-bin/astdys/astibo, accessed on 2008 December 1.

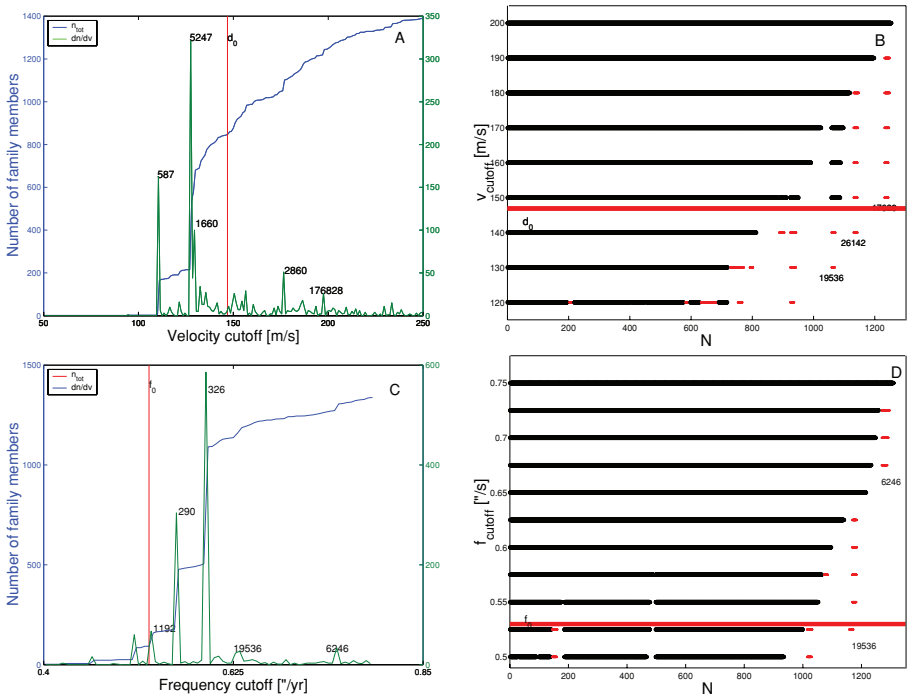

Figure 2. Panel A: the number and differential number of members of the classical Phocaea family as a function of the cut-off. The numbers on the peaks of the differential number of family members are related to the clusters that were englobed by the Phocaea family at higher velocity cut-offs. Panel B: a stalactite diagram of the Phocaea family region. Panels C and D: the same as panels A and B, but for the frequency groups.

To re-identify asteroid families, I also constructed a stalactite diagram in the traditional way defined by Zappalà et al. (1990) and Brož & Vokrouhlický (2008): I start with (25) Phocaea as the first central body and identify all the bodies associated with it at $d_{\rm cut-off} = 200\,{\rm m\,s^{-1}}$, a value for which no other independent cluster of asteroids was found in the Phocaea region. I then decrease the cut-off and identified the families and clumps among the asteroids not associated with (25) Phocaea. Fig. 2 (panel B) displays my results in the interval of cut-offs between 120 and 200 $\rm m\,s^{-1}$. Full black squares are associated with families in the region, and empty black squares are associated with clumps, according to the limits displayed in Fig. 1. Table 1 reports the families and clumps that I identified in this work. The first column reports if it is a family or a clump (the suffix c stands for groups identified in the proper element domain, while f stands for the groups found in the frequency space), the second column reports the lowest numbered asteroid in the group, the third reports the number of objects associated with the group, the fourth reports the number of object with spectral classification and the fifth reports the number of objects with SDSS-MOC4 data (see Section 3).

Table 1. Families and clumps in the region of the Phocaea group.

Id	Name	N	$N_{\rm spec}$	$N_{\rm SDSS-MOC4}$
Family(c)	(25) Phocaea	988	26	98
Family(f)	(25) Phocaea	1137	29	102
Family(c)	(19536) (1999 JM4)	27	0	3
Clump(f)	(19536) (1999 JM4)	14	0	2
Clump(c)	(17628) (1996 FB5)	10	0	0
Clump(c)	(26142) (1994 PL1)	10	0	1
Clump(f)	(6246) Komurotoru	9	0	1

To find the groups I used the following criterion. The clusters should be observable for a cut-off equal to d_0 and the 'length of the stalactite' associated with the family should be at least of 20 per cent of d_0, i.e. $\simeq 30\,{\rm m\,s^{-1}}$. The last requirement was set so as to avoid to identify as families sub-clusters of the Phocaea family that are eventually not connected to the family because of a conservative choice of the velocity cut-off. Based on the analysis of Fig. 2 (panel A), I choose to work with a cut-off of $160\,{\rm m\,s^{-1}}$, a value a bit larger than d_0 so as to include in the Phocaea family two small clusters [associated with (1963) Bezovec and (6487) Tonyspear]. With this choice of cut-off most of the Gil-Hutton families [such as the two families of (1660) Wood and (5247) Krylov] and clumps are now substructures of the Phocaea family. A new family associated with (19536) (1999 JM4) and two clumps associated with (17628) (1996 FB5) and (26142) (1994 PL1) were found in this work. The (19536) family picks the lower numbered asteroid (2860) Pasacentennium (former clump in Gil-Hutton 2006) at $v_{\rm cut-off} = 164\,{\rm m\,s^{-1}}$.

I then used the FHCM in the $(n, g, g-s)$ domain to identify members of the Phocaea dynamical family. Fig. 2 (panel C) displays the number of family members (left ordinate) and differential number ${\rm d}n/{\rm d}f$ (right ordinate) as a function of the frequency cut-off. The red vertical line displays the nominal frequency cut-off. The frequency family has only 92 members at the nominal frequency cut-off, and this fact may play against the possibility of using the nominal frequency cut-off for family determination in the frequency domain.

The numbers on the top of the peaks of differential asteroid numbers are related to the cluster of objects englobed by the Phocaea family at higher cut-offs. For $f_{\rm cut-off} = 0.530\,{\rm arcsec\,yr^{-1}}$ the Phocaea family conglomerates with the (1192) Prisma cluster, at $f_{\rm cut-off} = 0.560\,{\rm arcsec\,yr^{-1}}$ it merges with the (290) Bruna family, at $f_{\rm cut-off} = 0.595\,{\rm arcsec\,yr^{-1}}$ it coalesces with the (326) Tamara family, at $f_{\rm cut-off} = 0.625\,{\rm arcsec\,yr^{-1}}$ the family englobes the clump

associated with (19536) (1999 JM4), which is a family found in the proper element domain and, finally, at $f_{\rm cut-off} = 0.750$ arcsec yr^{-1} the family coalesces with the last clump, associated with (6246) Komurotoru, which is a clump only observed in the frequency domain. As observed for the classical family, there is no sudden fusion with the local background for higher values of the cut-off.

As done for the families in the proper element domain, I also constructed a stalactite diagram in the frequency domain. I follow a procedure similar to that described for the proper element groups, starting with a frequency cut-off of $f_{\rm cut-off} = 0.750$ arcsec yr^{-1}, for which no independent clump or family other than the Phocaea one could be identified in the region. Table 1 reports the families and clumps that were identified in the frequency domain. As observed in Fig. 2 (panel C), the value of the frequency cut-off needs to be at least larger than 0.595 arcsec yr^{-1}, or else the Phocaea family would be divided in two different groups. This value seems in agreement with that found in Carruba & Michtchenko (2009) for a smaller proper frequencies set. Information given by the stalactite diagram (Fig. 2, panel D) shows that the (19536) group, which was also identified in the proper element domain, is also distinguishable for $f_{\rm cut-off}$ larger than 0.525 arcsec yr^{-1} and smaller than 0.625 arcsec yr^{-1}. To obtain the larger possible sample of body in the Phocaea frequency family, I decided to work with a cut-off of 0.625 arcsec yr^{-1}.

An interesting feature observed at larger cut-offs is the clump around (6246) Komurotoru. This clump, which only coalesces with the Phocaea family for $f_{\rm cut-off} = 0.750$ arcsec yr^{-1}, is associated with the $(2\nu_6 - \nu_{16})$ resonance and is the first, to my knowledge, clump of object only detected in the frequency domain.[2] The clumps around (17628) and (26142), observed in the proper element domain, were not found in the proper frequency space.

To understand how the Phocaea family interacts with other families and clumps in the region, I also determined the local density of asteroids, following the approach of Carruba & Michtchenko (2009). Density maps will display regions characterized by strong mean-motion or secular resonances by a relatively low number of asteroids per unit bin. To quantitatively determine the local density of asteroids, I choose a region in the range of the a, e and $\sin(i)$ values of the local background for the Phocaea family as determined by Carruba & Michtchenko (2009). I computed the $\log_{10}$ of the number of asteroids per unit square in a 30 by 34 grid in a (starting at $a = 2.20$ au, with a step of 0.008 au) and e (starting at 0.08, with a step of 0.008). Results are shown in panel A of Fig. 3. Using similar procedures, I computed a density map of the Padua family region in the $(a - \sin(i))$ (Fig. 3, panel C), and $(g, g - s)$ (Fig. 3, panel E) planes. I choose to work with the $(g - s)$ plane because of the influence that the $(\nu_6 - \nu_{16})$ resonance exerts on the asteroids in the region (Carruba & Michtchenko 2009). Superimposed to the density maps I show projections of the Phocaea and (19536) families (as plus signs) and of the (17628) and (26142) clumps (as triangles, see also Table 1 for information on the families and clumps) obtained in the proper element domain. Since the number density of objects in this area is relatively low, I did not use the median filter described in Carruba et al. (2004) to smooth out the effects of three-dimensional projections in 2D planes, binning, etc.

[2] At a cut-off of 0.625 arcsec yr^{-1} the clump has nine members, which is slightly below the criterion used to identify clumps for this cut-off (11 members). Since the clump is robust at higher cut-offs, I decided to accept it at 0.625 arcsec yr^{-1} as well.

As already discussed in Carruba & Michtchenko (2009), note how the Phocaea family is surrounded by a region with a very low density of asteroids. The Phocaea family seems essentially to fill all the available space in the 'stable island' region between secular and mean-motion resonances. This might either suggest that the family is an artefact of the dynamics in the region, rather than be an actual collisional family, or that it is an actual family leaking members to the local web of powerful mean-motion and secular resonances. I will come back to the subject in Section 8. Also note how in the $(g, g - s)$ space several members of the family are aligned inside the $(\nu_6 - \nu_{16})$ resonance at $g - s = 54.588$ arcsec yr^{-1}. Since the family strongly interacts with a resonance of argument $(g - s)$, Carruba & Michtchenko (2009) suggested to look for families in the region in the $(n, g, g - s)$ domain.

For what concerns the frequency groups, in Fig. 3, I show (a, e) (panel B), $(a, \sin(i))$ (panel D) and $(g, g - s)$ (panel F) projections of the frequency family and clumps, superimposed with the density map obtained for the classical case. Note how the frequency Phocaea family is much more extended along the $(\nu_6 - \nu_{16})$ resonance than the corresponding Phocaea classical family [see Fig. 3 (panel F), Fig. 3 (panel E) and the discussion in Carruba & Michtchenko (2009) for a quantitative estimate of the efficiency of the metric in the $(n, g, g - s)$ domain in obtaining members of families interacting with such resonances].

Also, note how the Komurotoru clump is essentially aligned with a strip at $\simeq 63$ arcsec yr^{-1} in the $(g - s)$ variable. In Section 8, I will show how this region is associated with the $(2\nu_6 - \nu_{16})$ secular resonance. In the following sections, I will further analyse the families obtained in the proper element and frequency domain in terms of compositional analysis.

3 THE COMPOSITIONAL ANALYSIS

As a preliminary step in the analysis of the Phocaea family, I reviewed the current knowledge about the taxonomical classification of members of the frequency Padua family. Using the data present in the three major photometric/spectroscopic surveys Eight-Colour Asteroid Analysis (ECAA; Zellner, Tholen & Tedesco 1985; Tholen 1989), Small Main Belt Spectroscopic Survey (SMASS; Xu et al. 1995; Bus & Binzel 2002a,b) and Small Solar System Objects Spectroscopic Survey (S3OS2; Lazzaro et al. 2004), I identified in the Phocaea family background (defined as in Carruba & Michtchenko 2009) four A-type, one L-type, 36 S-type, two X-type, four C-type and three D-T-type objects. Of these, 26 were members of the Phocaea classical family and seven were members of the Phocaea frequency family (but not of the classical one; vice versa there were four objects that were members of the classical family but not of the frequency one). Table 2 reports the asteroid identification, family status (c stands for the classical family, and f for the frequency one), geometric albedo, diameter and spectral class for the asteroids for which at least some of this information is available. Data on the albedo and asteroid diameters for which an error estimate was available was taken from Tedesco et al. (2002) (see also Section 3). Data on the albedo for which an error estimate is not available were from the Horizon web site (http://ssd.jpl.nasa.gov).

Carvano et al. (2001) analysed 31 objects in the Phocaea region (as well as 29 asteroids in the Hungaria group) and concluded that, despite the presence of a large C-type object in the family, (105) Artemis, the fact that the majority of asteroids was tightly concentrated in the region of the Phocaea family suggested that the family could be a real product of a collisional outbreak. Fig. 4 displays an (a, e) (panel A), $(a, \sin(i))$, (panel B), $(e, \sin(i))$

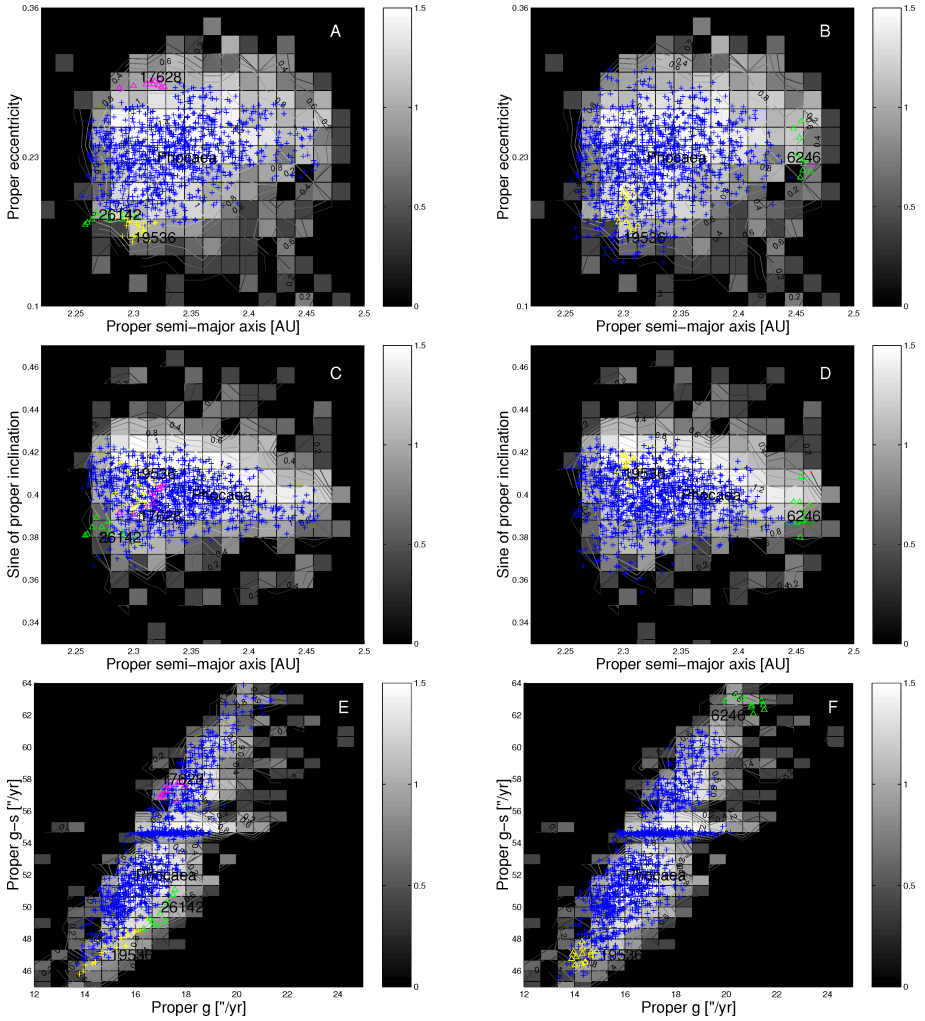

Figure 3. An $(a - e)$ (panel A), $(a - \sin(i))$ (panel C) and $(g, g - s)$ (panel E) projections of the families and clumps (see Table 1) in the region of the Phocaea family, obtained in the proper element domain. Panels B, D and F display the same, but for the groups obtained in the $(n, g, g - s)$ frequency domain.

(panel C) and $(g, g - s)$ (panel D) projections of the asteroids with a known spectroscopical classification, along with the members of the Phocaea frequency family (blue dots).

As can be seen in Fig. 4, and from the data of Table 2, all C-type asteroids in the region are not members of the Phocaea families, including (105) Artemis. Most of the S-type objects in the region were members of the Phocaea families, with six exception. There were only three members of the family with types other than S: (950) Ahrens (A-type, not incompatible with the mineralogy of an S-type family), (1318) Nerina (X-type) and (4666) Dietz (D-T type). The ratio of 9.1 per cent of objects with a spectral type different than the dominant one seems to be compatible with the expected ratio of interlopers for a family of the size of Phocaea (Migliorini et al. 1995, but the sample of objects with a known spectral type is still too small to reach a definitive conclusion).

For the purpose of extending the sample for which information on taxonomy is available, I turn my attention to the SDSS-MOC4 data. The SDSS MOC4 lists astrometric and photometric data for asteroids observed by the 2.5-m Sloan telescope located at Apache Point Observatory, in Sunspot, New Mexico. To date (fourth release), the survey has determined positions, brightness, and five-colour CCD photometry of 471 569 moving objects (Parker et al. 2008).

The flux reflected by the detected objects was measured almost simultaneously in five bands (measurements in two successive bands were separated in time by 72 s) with effective wavelengths 3557 Å (u band), 4825 Å (g band), 6261 Å (r band), 7672 Å (i band) and 9097 Å (z band), and with 0.1–0.3 μm band-widths (Fukugita et al. 1996). Here I follow the approach of Roig & Gil-Hutton (2006) to obtain principal components in the space of albedos F_u, F_g, F_i, F_z. Using the criteria introduced by Roig & Gil-Hutton (2006) to reject data with large errors, I obtain a data set of 18 178 objects with principal components data, 17 258 of which are related to numbered objects.

Once the two first principal components are found, the data can be used to classify asteroids according to their taxonomic types and to determine asteroid families in the space of proper elements and colours simultaneously. Bus & Binzel (2002a,b) and Nesvorný et al. (2005) introduced the following extended metrics in this space:

$$d_3 = \sqrt{d^2 + C_{\rm PC}[(\delta {\rm PC}_1)^2 + (\delta {\rm PC}_2)^2]}, \quad (3)$$

where d is the distance given by the standard metric of Zappalà et al. (1995), and $\rm PC_1$ and $\rm PC_2$ are the two first principal components. Carruba & Michtchenko (2007, equation 3) also introduced metrics of colours and frequencies in the $(n, g, g + s, {\rm PC}_1, {\rm PC}_2)$

Table 2. Asteroids in the Phocaea region with known spectral classification.

Number	Name	Family membership	Albedo	Diameter (km)	Spectral type
25	Phocaea	Phocaea c,f	(0.2310 ± 0.024)	(75.13 ± 3.6)	S
105	Artemis		(0.0465 ± 0.002)	(119.08 ± 2.8)	C
265	Anna		(0.1045 ± 0.033)	(23.66 ± 3.0)	X
273	Atropos		(0.1624 ± 0.015)	(29.27 ± 1.3)	L
323	Brucia	Phocaea c,f	(0.1765 ± 0.018)	(35.82 ± 1.7)	S
391	Ingeborg				S
502	Sigune	Phocaea c,f	(0.3405 ± 0.105)	(15.98 ± 2.0)	S
654	Zelinda		(0.0425 ± 0.003)	(127.40 ± 3.9)	C
914	Palisana		(0.0943 ± 0.004)	(76.61 ± 1.7)	C
950	Ahrensa	Phocaea f	(0.1793 ± 0.054)	(15.03 ± 1.8)	A
1090	Sumida				D-T
1108	Demeter		(0.0464 ± 0.008)	(25.61 ± 2.0)	C
1164	Kobolda	Phocaea c,f			S
1316	Kasan				A
1318	Nerina	Phocaea c,f	(0.1811 ± 0.017)	(13.02 ± 0.6)	X
1322	Coppernicus				S
1367	Nongoma	Phocaea c			S
1568	Aisleen	Phocaea c,f			S
1573	Vaisala	Phocaea f	(0.2226 ± 0.043)	(9.77 ± 0.8)	S
1575	Winifred	Phocaea c,f	0.2452	9.3	S
1591	Baize	Phocaea c,f	0.1056	18.7	S
1660	Wood	Phocaea c,f			S
1816	Liberia	Phocaea c,f			S
1883	Rimito	Phocaea c,f			S
2014	Vasilevskis	Phocaea c,f			S
2050	Francis	Phocaea f			S
2105	Gudy		(0.1078 ± 0.007)	(22.25 ± 0.7)	D-T
2430	Bruce Helin	Phocaea f			S
2791	Paradise				A
2965	Surikov				S
3267	Glo	Phocaea c,f	0.0607	13.6	S
3343	Nezdel				S
3388	Tsanghinchi	Phocaea c,f			S
3792	Preston	Phocaea f			S
3888	Hoyt	Phocaea c,f			S
3913	Chemin	Phocaea c,f			S
4103	Chahine		(0.3477 ± 0.027)	(12.97 ± 0.5)	A
4121	Carlin	Phocaea c,f	(0.4164 ± 0.086)	(6.82 ± 0.6)	S
4132	Bartok	Phocaea c,f	(0.3308 ± 0.039)	(10.5 ± 0.6)	S
4340	Dence				S
4511	Rembrandt	Phocaea c,f	(0.2861 ± 0.066)	(9.02 ± 0.9)	S
4533	Orth	Phocaea c,f			S
4666	Dietz	Phocaea f			D-T
4826	Wilhelms	Phocaea c,f			S
4995	Griffin	Phocaea c,f			S
5647	(1990 TZ)	Phocaea c	(0.4729 ± 0.072)	(10.62 ± 0.7)	S
6084	Bascom	Phocaea f			S
6560	Pravdo				S
6847	Kunz-Hallstein	Phocaea c,f			S
11548	Jerrylewis	Phocaea c			S

domain. Since in this work, I am interested in studying the interaction of asteroids with a resonance of argument $(g - s)$, it is more appropriate to use a metric in the $(n, g, g - s, \mathrm{PC}_1, \mathrm{PC}_2)$ domain of the form

$$d_4 = \sqrt{f^2 + D_{\mathrm{PC}}[(\Delta \mathrm{PC}_1)^2 + (\Delta \mathrm{PC}_2)^2]}, \quad (4)$$

where f is the distance metric in the frequency domain given by equation (2), and D_{PC} is a numerical factor, empirically set equal to 200 to give comparable results for the typical differences in proper frequencies and those in principal components.

Following the approach of Carruba & Michtchenko (2007), I selected an S-type asteroid in the Phocaea classical and frequency families also present in the 17 258 data base of numbered asteroids for which data on PC_1 and PC_2 are available: (4132) Bartok. A similar procedure was carried out for the families and clumps obtained in the proper element domain for which at least one member had principal component data. I found that for a cut-off of 380 m s^{-1} the (19 536) family coalesces with the Phocaea family, and therefore I decided to work with a cut-off of 375 m s^{-1}. At this cut-off I found that the Phocaea family has 112 members, the (19 536) family has 11 members and the (26 142) clump has one member [no

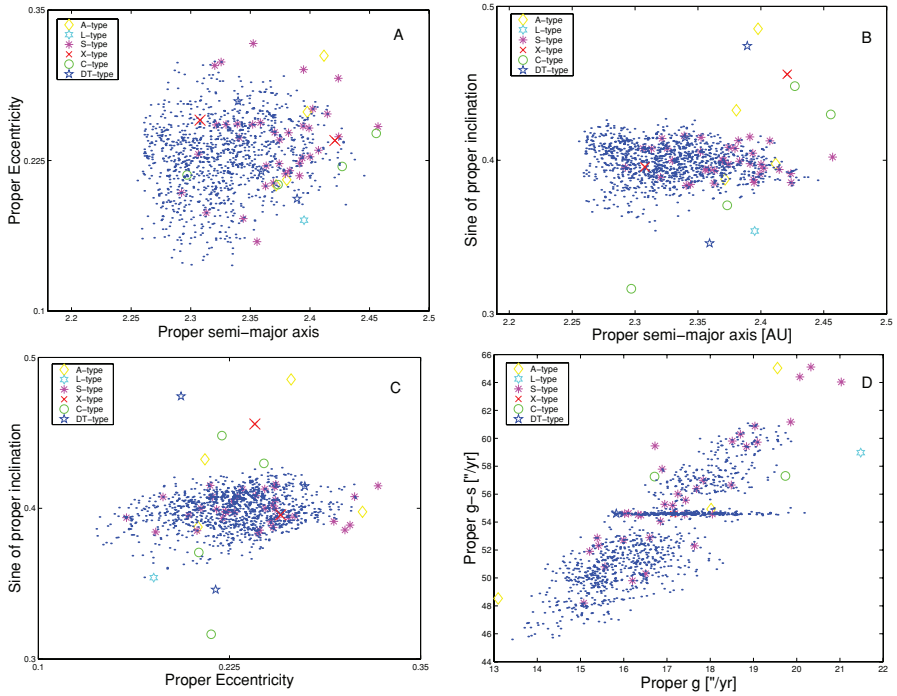

Figure 4. Taxonomic distribution of asteroids in the region of the Phocaea family.

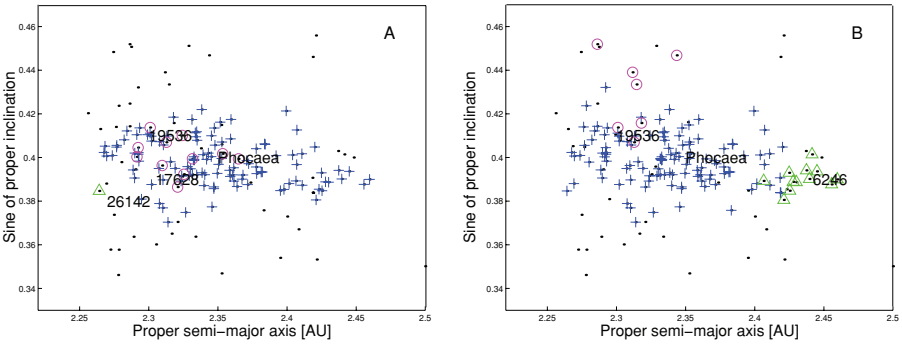

Figure 5. Panel A: an $(a, \sin(i))$ projection of the members of the Phocaea, (blue crosses), (19 536) (magenta circles) and (26 142) (green triangle) dynamical groups found in the space of proper element and principal components. Black dots display the location of asteroids in the SDSS-MOC4 data base in the region. Panel B: the same for members of the Phocaea (blue crosses), (19 536) (magenta circles) and (6246) (green triangles) found in the space of proper frequencies $(n, g, g - s)$ and principal components.

member with principal component data was found for the (17 628) clump].

Fig. 5 (panel A) displays a projection of the members of the Phocaea, (blue crosses), (19 536) (magenta circles) and (26 142) (green triangle) dynamical groups found in the space of proper element and principal components. Black dots display the location of asteroids in the SDSS-MOC4 data base in the region. As can be seen in the figure, the orbital distribution of the Phocaea family members found in the domain of proper elements and principal components follows quite closely the distribution of the family members in the space of proper elements (see Fig. 3, panel C).

I then obtained families and clumps in the domain of proper frequencies and principal components using equation (4). For a cut-off of 2.3 arcsec yr^{-1} the (6246) Kunamoto cluster merges with the Phocaea family, so I decided to work with a cut-off of 2.2 arcsec yr^{-1}. At this cut-off, the Phocaea family has 115 members, the (19 536) clumps have seven members and the (6246) clump has 12 members.

Fig. 5 (panel B) displays a projection of the members of the Phocaea, (blue crosses), (19 536) (magenta circles) and (6246) (green triangle) dynamical groups found in the space of proper frequencies and principal components. As can be seen in the figure, the orbital distribution of the Phocaea family members follows closely that of the family found in the space of proper frequencies (see Fig. 3, panel D). The 19 536 clump found in the domain of proper frequencies and principal components is, however, extended at higher $\sin(i)$ values with respect to the clump obtained in the space of proper frequencies only. The (6246) Kunamoto clump is extended at smaller values of the semimajor axis with respect to the one found in the space of proper frequencies only, and merges with the Phocaea family for slightly larger values of the frequency cut-off. In the next section, I will investigate the values of albedo and

absolute magnitudes for asteroids in the region that are available in the literature.

4 GEOMETRIC ALBEDOS AND ABSOLUTE MAGNITUDES

The cumulative size distribution of asteroid family members can be used to obtain important information about the collisional and orbital evolution of asteroid families (Vokrouhlický et al. 2006a,b,c). Estimates of the asteroid diameters can be obtained via the relationship

$$D = \frac{D_0}{\sqrt{p_V}} \times 10^{-0.2H}, \quad (5)$$

where $D_0 = 1329$ km, H is the asteroid absolute magnitude and p_V is the geometric albedo. To obtain reliable estimates of the diameters of asteroids, it is therefore important to first obtain good values of the asteroids geometric albedos and absolute magnitudes. For what concerns the asteroids albedos, I turn my attention to the work of Tedesco et al. (2002), which reported the values of geometric albedo (with their uncertainties) for 2226 bodies. Of these, I found 33 objects in the region of the local background of the Phocaea frequency family (Carruba & Michtchenko 2009), for which synthetic proper elements were also available. 11 of these objects belong to either the Phocaea classical or frequency families and have a reported spectral classification.

Fig. 6 (panel A) displays an $(a, \sin(i))$ projection of the Phocaea frequency family (small blue dots) and of the 33 objects with albedos in the region. Asteroids with albedos lower than 0.10 (usually associated with C-type bodies) are displayed with small black dots, those with albedos between 0.10 and 0.25 (associated with S-type objects, Bus & Binzel 2002a,b) are shown with larger red dots, and asteroids with albedos larger than 0.25 are displayed with large full yellow dots. As can be seen in the figure, most of the objects with low albedos are found outside the family, and there is a concentration of the objects with an S-type compatible albedo in the region of the Phocaea family, so confirming the possible interpretation of the family as being the product of the disruption of a large S-type parent body. I however also observe some high-albedo objects that are associated with the family. This is more evident in Fig. 6 (panel B) where I show a histogram of the normalized number of objects in the albedo intervals 0.00–0.10 (C-type), 0.10–0.25 (S-type) and larger than 0.25, for all asteroids in the region (blue line) and just for the Phocaea families members (red line). While only a member of the Phocaea family has low albedo, there were five objects, all with diameters of 10 km or less, with albedo larger than the value usually associated with S-type bodies.

Taking the median value of the Phocaea member albedo, and using the standard deviation as a measure of its error, I found that the albedo values of the Phocaea members lie in the interval $p_V = (0.24 \pm 0.12)$. For what concerns the asteroids absolute magnitudes, Fig. 7 displays $(a - e)$ (panel A), $(a - \sin(i))$ (panel B), $(e - \sin(i))$ (panel C) and $(g, g - s)$ projections of the asteroids in the region of the Phocaea family. Small black dots display the locations of asteroids with $H > 12$, red full dots are associated with asteroids with $10 < H < 12$ and large yellow dots display the position of all objects with magnitude smaller than 10.

As can be seen in the figure, the distribution of bodies is not symmetrical about the semimajor axis, with respect to the centre of the family. There is an excess of objects at the lower semimajor axis with respect to the distribution at higher a. Three large C-type objects, (105) Artemis, (654) Zelinda and (914) Palisana are present in the region but are not connected to the Phocaea dynamical family, as discussed in the previous sections. The family of (25) Phocaea itself sits on the separatrix of the $(\nu_6 - \nu_{16})$ secular resonance. Medium-sized bodies are generally associated with the family. More information on the size distribution of the Phocaea family will be discussed in Section 6.

5 YARKOVSKY ISOLINES AND *C*-TARGET FUNCTION

Now that I have already revised the information on the literature on geometric albedos and absolute magnitude, I am equipped to start setting constraint on an age estimate for the Phocaea family. In Vokrouhlický et al. (2006a,b) the authors used the (a, H) distribution of asteroid families to determine their ages. In particular, the authors introduced a target function C defined as

$$0.2H = \log_{10}(\Delta a / C), \quad (6)$$

where $\Delta a = a - a_c$, and a_c is the 'central' value of the semimajor axis of the family members. The most appropriate definition of family centre relates to the concept of barycentre. I took

$$a_c = \sum_{i=1}^{n_{ast}} \frac{a \times M_i}{M_{tot}}, \quad (7)$$

where n_{ast} is the number of family members and M_i is the mass of each asteroid, estimated by assuming that all asteroids can be approximated as spheres, using a density of 2500 kg m^{-3}, typical of S-type objects, and a diameter obtained using equation (5). For

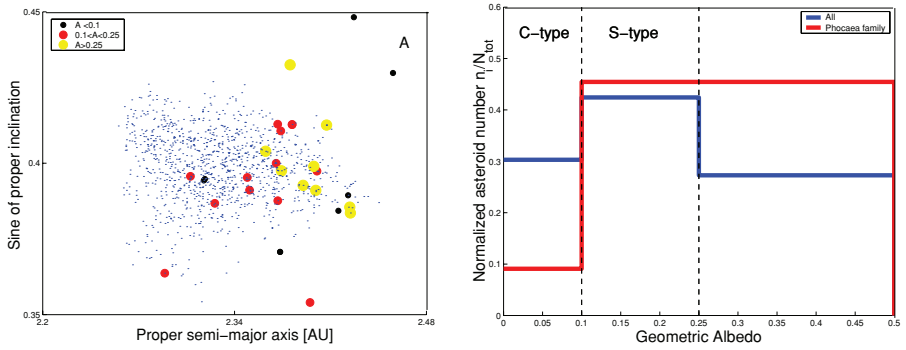

Figure 6. Panel A: an $(a, \sin(i))$ projection of the orbital location of asteroids for which a value of the geometric albedo is available in the region of the Phocaea family. Panel B: histogram of the normalized number of objects per unit bins in the albedo intervals 0.00-0.10 (C-type), 0.10–0.25 (S-type) and larger than 0.25, for all asteroids in the region (blue line) and just for the Phocaea families members (red line).

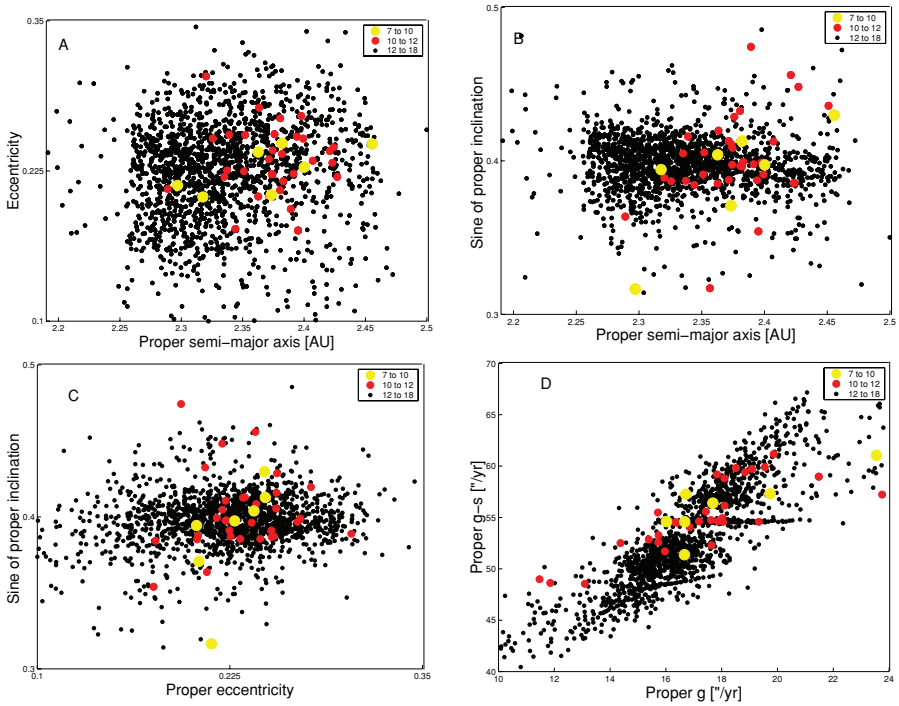

Figure 7. An $(a - e)$ (panel A), $(a - \sin(i))$ (panel B), $(e - \sin(i))$ (panel C), and $(g, g - s)$ projections of the asteroids in the region of the Phocaea family. Small black dots display the locations of asteroids with $H > 12$, red full dots are associated with asteroids with $10 < H < 12$ and large yellow dots display the position of all objects with magnitude smaller than 10.

asteroids for which the geometric albedo is not available, I used the average value of albedo for the Phocaea family, $p_V = 0.24$. Equations similar to equation (7) hold for e_c and i_c. With these approximations, I found that the total mass M_{tot} of the classical family is of the order of 2.35×10^{18} Kg, 34.7 per cent of which is contained in (25) Phocaea. The total mass of the frequency family is of the order of 2.88×10^{18} Kg, 28.3 per cent of which is contained in (25) Phocaea. The barycentre of the classical family is located at $a_c = 2.3851$ au, $e_c = 0.2373$ and $i_c = 23^{\circ}.8433$, while that of the frequency family is located at $a_c = 2.3497$ au, $e_c = 0.2151$ and $i_c = 23^{\circ}.3117$.[3] For what concerns the a_c value obtained for the frequency family, I notice that the frequency family is seriously depleted beyond higher values of a with respect to the M1:-2A resonance with Mars. As a consequence, the value of the family barycentre is displaced at lower a with respect to that of the classical family. For this reason, I choose to work essentially with the barycentre of the classical family.

As part of my preliminary analysis of the Phocaea family I show (a, H) and $(g - s, H)$ projections of the members of the frequency Phocaea family. Results are similar for the classical family. For what concerns the (a, H) projections, I also show the distance covered by the asteroids to diffuse from the centre of the family via the Yarkovsky effect, computed using the Vokrouhlický (1998) model of the diurnal version of the Yarkovsky effect, for spherical bodies and in the linear approximation for the heat conduction in a spherical, solid and rotating body illuminated by solar radiation. I used the following parameters to describe the Yarkovsky force: a value of thermal conductivity $K = 0.0001$ W m^{-1} K^{-1}, a specific heat capacity of $C_p = 680$ J kg^{-1} K^{-1}, a density of 2500 g cm^{-3}, a surface density of 1500 g cm^{-3}, a bond albedo of 0.11 and a geometric albedo of 0.24 (see Section 4 for a discussion on the geometric albedo data). With these parameters, using the barycentric value of the family a distribution a_c, and assuming a rotation period inversely proportional to the radius (Farinella, Vokrouhlický & Hartmann 1998), I obtained lines of maximal Yarkovsky drift for the Phocaea frequency (Fig. 8, panels A) members, for ages of 1500 and 2200 Myr. Since I am not considering the effect of the primordial ejection velocity field, this sets upper limits on the possible age of the family. My preliminary analysis seems to confirm the possibility that the Phocaea family is indeed a very old one. Also notice how both classical and frequency families (and more so for the frequency family) are depleted in members for values of the semimajor axis larger than the family barycentre. This is most likely caused by the local dynamics, and in particular by the direct and indirect effect of the strong ν_6 secular resonance. More information on the local dynamics can be found in Section 8.

Another interesting piece of information can be obtained by observing the $(g - s, H)$ projection of the frequency family (Fig. 8). Note that the central strip of the family members is locked in the $(\nu_6 - \nu_{16})$ secular resonance. Contrary to the case of the Padua family (Carruba 2009), however, only 112 members of the classical family (11.33 per cent of the total members) and 120 of the frequency family (10.55 per cent of the family total) are locked in this resonance (more than 75 per cent of the Padua family members were locked in the z_1 resonance). The fact that the majority of the members of the family are not in the resonant configuration is reflected by the fact that the family is characteristically dispersed in 'triangle diagrams'. The role of the $(\nu_6 - \nu_{16})$ secular resonance is therefore more limited for the case of the Phocaea family than the one played by the z_1 resonance for the Padua family. Finally, the lack of objects in the frequency family with values of $(g - s)$ higher than

[3] The mean values of the family semimajor axis, eccentricity and inclination are $a_c = 2.3348$ au, $e_c = 0.2328$ and $i_c = 23^{\circ}.5143$ for the classical family, and $a_c = 2.3284$ au, $e_c = 0.2280$ and $i_c = 23^{\circ}.4883$, for the frequency one.

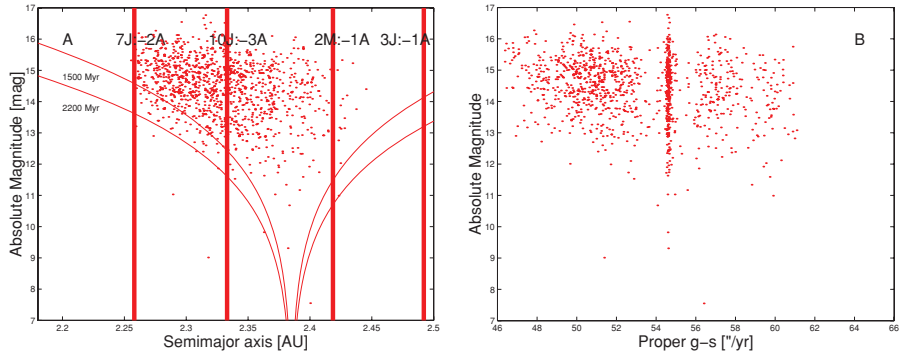

Figure 8. An (a, H) (panel A) and $(g + s, H)$ (panel B) projection of the members of the frequency Phocaea family.

61.5 arcsec yr^{-1} is caused by the barrier in the frequency domain presented by the M1:-2A resonance with Mars (see Section 8).

The asymmetry between the population of objects at lower and higher a is also observed if we compute the C-target function.[4] Positive values of C are significantly depleted and I do not observe a peak at $C > 0$. I believe this asymmetry can be explained in terms of the local dynamics, as discussed above. More information on secular and mean-motion resonances in the region will be given in Section 8.

6 CUMULATIVE DISTRIBUTION AND COLLISION PROBABILITIES

The size distribution of asteroids is one of the most significant observational constraints on their history, and it is also one of the hardest quantities to determine because of strong selection effects (Parker et al. 2008). As a next step of my preliminary analysis of the Phocaea family, I compute the cumulative H distribution $N(<H)$ for the two Phocaea families, the classical (Fig. 9, panel A) and the frequency one (Fig. 9, panel B). As it is the case for several other families studied by Parker et al. (2008), the Phocaea family cumulative distribution seems to be best approximated by a 'broken' power law, for the two intervals in H between 12 and 14 and between 14 and 15. I found that for the classical family, the γ exponents that best fit the two intervals are 0.60 and 0.35, respectively, while for the frequency family I obtained values of γ of 0.53 and 0.32. The γ exponents found for the first interval are compatible with the 0.61 γ value for background population found by Parker et al. (2008) for the inner main belt, but the values found for the second intervals seem quite low and may indicate that there was a significant depletion in the population of smaller objects in the area.

In Fig. 9 (panels C and D), I show the dependence of the exponent of the cumulative H distribution $N(<H)$ as a function of the velocity and of the frequency cut-offs, found in the range of the absolute magnitude of H (12.5, 14.0) (red lines) and (14.0, 15.0) (blue lines). Vertical lines display the values of the cut-offs for which the Phocaea family englobes other families and clumps in the region (see Fig. 2, panels A and C). As can be seen in the figure, the cumulative exponents fluctuate when the Phocaea cluster englobes some of the minor group in the region and then practically reach a constant value for larger cut-offs. The fact that the exponents do not drop at very large cut-off, i.e. when the whole background zone becomes associated with the family (Vokrouhlický et al. 2006b), is caused by the fact that I obtained the Phocaea (and the other groups in the region) using a sample with only the asteroids in the Phocaea family local background (Carruba & Michtchenko 2009). Apparently the local background of the Phocaea family is actually dominated by Phocaea family members (plus the odd large C- and X-type asteroids; see Section 3). As soon as the Phocaea family reaches the dynamical limits of the stable island, it essentially stops to grow significantly, and so the cumulative exponents essentially stop varying.

One question that may arise at this point regards the possibility that the Phocaea family was created by a collision and it is therefore an actual family, rather than a dynamical group limited by the 'stable island' region. To start investigating the possible role that asteroids in different regions may have had in the collisional evolution of the Phocaea family, I used the approach of Greenberg (1982) for obtaining intrinsic collision probabilities of members of the Phocaea classical family with (25) Phocaea itself, an asteroid in the inner main belt, (8) Flora and an asteroid in the middle belt, (15) Eunomia.

Values of collision probabilities are actually in general higher for the interaction of asteroids with (8) Flora than with (25) Phocaea itself. The average value of P for collisions with (8) Flora was of 8.2×10^{-18} km^{-2} yr^{-1}, while that with (25) Phocaea was of 10.9×10^{-18} km^{-2} yr^{-1}. For comparison, the average value of P with (15) Eunomia was of 4.8×10^{-18} km^{-2} yr^{-1}, while the average probability of two main belt asteroid to collide is of 2.8×10^{-18} km^{-2} yr^{-1}. This simple test may indicate that collision with inner main belt, low-inclination objects may have certainly played a role in the collisional history of the Phocaea family, but a further, more in-depth, study is needed to clarify this point.

As an order of magnitude estimate for the age of the Phocaea family, let us assume a value of the collision probability of the impact of $a \simeq 10$ km size projectile of $P_i \simeq 10^{-17}$ km^{-2} yr^{-1}. The disruption of a parent body of 120–150 km would have a characteristic time-scale of

$$\tau \simeq \frac{1}{(P_i(R_t + R_p)^2)N_p)}, \tag{8}$$

where N_p is the number of projectiles in the main belt (between 5000 and 10 000 according to Bottke et al. 2005), R_t is the target radius (of the order of 60 km) and R_p is the projectile radius (of the order of 5 km). Assuming an optimistic value for the number of projectiles in the main belt, this supports a 2.4 Byr estimate for the collisional age of the Phocaea family, in agreement with the estimates obtained in Section 5.

[4] I computed the observed data $N_{\rm obs}(C)$ for the classical and frequency families, obtained by $(C, C + \Delta C)$ binning with $\Delta C = 4.0 \times 10^{-6}$ and $a_c = 2.3851$ au (the barycentre of the classical family).

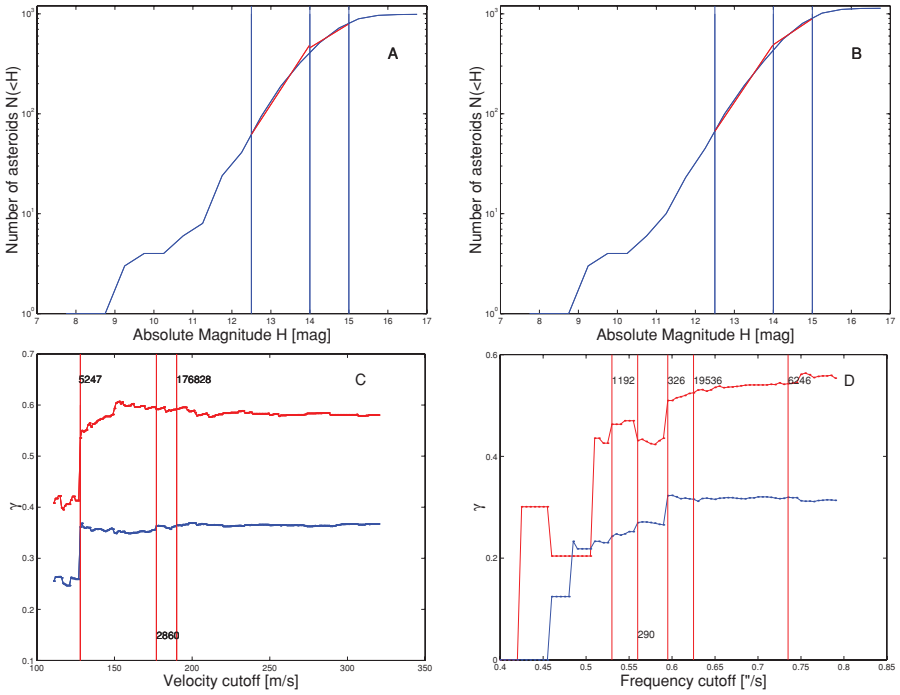

Figure 9. Panels A and B display the cumulative distribution $N(>H)$ of the classical and frequency members of the Phocaea family. Panels C and D display the dependence of the exponent of the cumulative H distribution $N(<H)$ as a function of the velocity and of the frequency cut-offs, found in the range of absolute magnitude H (12.5, 14.0) (red lines) and (14.0, 15.0) (blue lines).

7 LIGHT CURVE AND ROTATION RATE ANALYSIS

It has been recently proposed that binary asteroids can be formed because of the increase in the rotation rate of the parent body caused by the Yarkovsky-O'Keefe-Radzievskii-Paddack (YORP) effect (Pravec et al. 2008). Obtaining information on the asteroid periods is therefore of significant importance in understanding their dynamical evolution. Here I revised the current information available for members of the Phocaea classical and frequency families in the Asteroid Light-Curve Data Base (LCDB; Warner, Harris & Pravec 2008) as of 2009 March. There are a total of 1213 asteroids between the Phocaea classical and frequency family. Of these, 18 had a period estimate in the LCDB.

Fig. 10 displays a histogram of the distribution of rotation frequencies for the 18 asteroids for which such information is available.

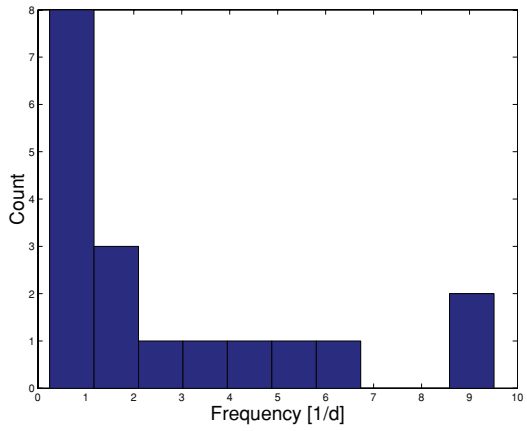

Figure 10. Histograms of rotation frequencies (in d^{-1} for the 18 Phocaea families members present in the Asteroid Light-Curve Data Base.

The sample is too limited to allow to obtain statistically significant information, but it can be noticed that there are two objects, (2000) Herschel and (4283) Stoffler, with periods longer than 50 h, and eight objects with periods longer than 1 d. As found by Warner et al. (2009) for asteroids in the Hungaria region, there seems to be an excess of slow rotators, while the distribution of spin rates in the range of $1\mathrm{d}^{-1} < f < 7\mathrm{d}^{-1}$ appears to be uniform. This can be possibly caused by the YORP effect, with the excess of slow rotators related to the longer time slowly rotating objects spend in that state (Pravec et al. 2008).

8 DYNAMICS IN THE REGION OF THE PHOCAEA FAMILY

As discussed in Knežević & Milani (2003), the Phocaea family is characterized by a region of shallow close encounters with Mars at $e > 0.3$, which displays significant chaotic behaviour. To further study and delimit this region it is useful to compute maximum Lyapunov exponents (MLE) for orbits in this area. A detailed explanation of the theory of Lyapunov exponents goes beyond the scope of this paper; instead, I refer the reader to Lyapunov (1907) and Benettin et al. (1980). The MLE is a measure of exponential stretching of nearby orbits. The Lyapunov exponents are equal to zero for regular orbits (they tend to zero in finite-time calculations), while they assume positive values for chaotic orbits. The inverse of a Lyapunov exponent is the Lyapunov time T_L. Smaller values of T_L indicate enhanced local stochasticity.

I start my analysis by looking at the values of MLEs currently available in the AstDyS data base in the Phocaea family region. Fig. 11 displays an $(a - e)$ (panel A), $(a - \sin(i))$ (panel B), (a, q) [panel C, where $q = a\,(1 - e)$ is the asteroid pericentre] projections of asteroid Lyapunov times in the region of the Phocaea family. Small black dots have Lyapunov times smaller than 20 000 yr, large

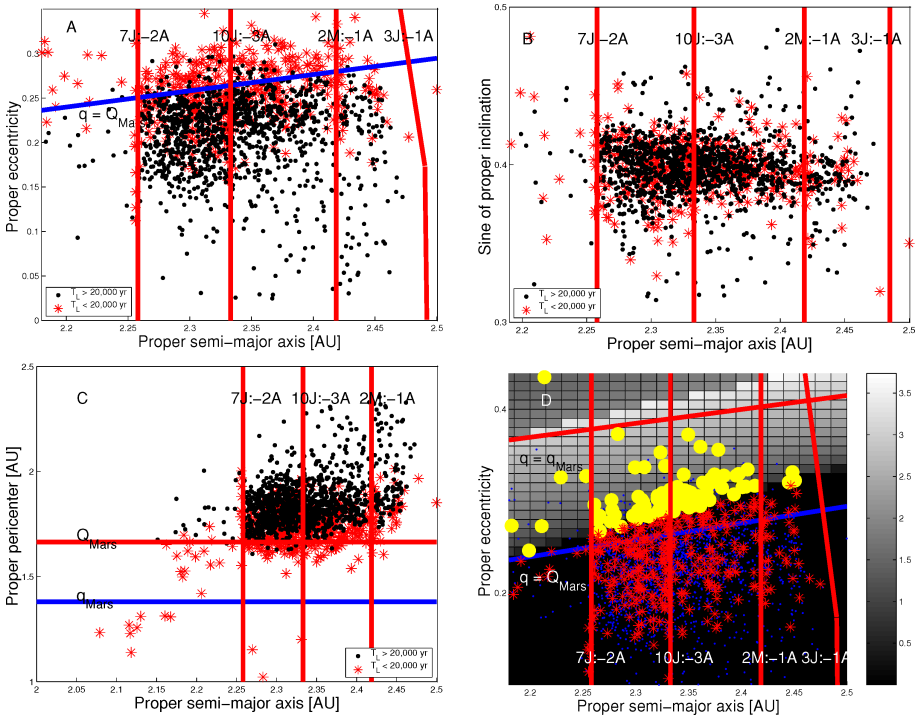

Figure 11. An (a, q) (panel A), $(a, \sin(i))$ (panel B), (a, q) (panel C) projection of asteroids Lyapunov times in the region of the Phocaea family. Small black dots have Lyapunov times smaller than 20 000 yr, large red asterisks have $T_L < 20\,000$ yr. Panel D displays an (a, e) projection of asteroids in the region of the Phocaea family (blue dots), superimposed with a colour plot of $[(\langle \Delta a^2 \rangle T)^{1/2}] \times 10^3$ caused by encounters with Mars. Full red dots are asteroids with Lyapunov times T_L smaller than 20 000 yr, and full yellow dots are asteroids with $T_L < 20\,000$ yr and $(\langle \Delta a^2 \rangle T)^1/2 > 0$.

red asterisks have $T_L < 20\,000$ yr. Panel C of Fig. 11 displays the MLE versus the asteroid pericentre. Vertical lines show the values of q equal to Mars pericentre (blue line) and apocentre (red line).

As can be seen in Fig. 11 (panel A), orbits with small Lyapunov times are generally (but not only) characterized by larger values of eccentricity, roughly speaking $e > 0.22$. The blue line in the figure displays the location of asteroids with the pericentre equal to the apocentre of Mars, which have the potential to be Mars crossers. With the exception of asteroids interacting with the 7J:-2A, the 2M:-1A or other mean-motion and secular resonances, most of the asteroids with low Lyapunov times are either Mars crossers or are objects that can be perturbed by encounters with Mars. This is more clearly shown in Fig. 11 (panel C), where I see that the lowest values of Lyapunov times are associated with Mars-crosser bodies. Note how there is no particular correlation between Lyapunov times and inclination (Fig. 11, panel B). This is also observed in the space of asteroid proper frequencies.

To further study the effect of close encounters with Mars on chaos in the Phocaea region, I turn my attention to the work of Greenberg (1982) on orbital interaction during close encounters. In his work, Greenberg assumed that the gravitational interaction between two closely approaching orbiting bodies can be modelled as a two-body hyperbolic encounter. As in Carruba et al. (2003), I used this approach to compute $(\langle \Delta a^2 \rangle\ T)^{1/2}$ (where Δa is the change in the semimajor axis and T is the orbital period of the perturbee, of the order of 3.72 yr) for a grid of particles in the (1.9–2.5) au range in a, (0–0.43) range in e and with the inclination equal to that of (25) Phocaea at J2000 (23°.414). I also computed the same quantity for all the 1736 objects in the local background of the Phocaea family. Fig. 11 (panel D) displays an (a, e) projection of asteroids in the region of the Phocaea family (blue dots), superimposed with a colour plot of $[(\langle \Delta a^2 \rangle\ T)^1/2] \times 10^3$ caused by encounters with Mars. Red asterisks are asteroids with Lyapunov times T_L smaller than 20 000 yr, and full yellow dots are asteroids with $T_L < 20\,000$ yr and $[(\langle \Delta a^2 \rangle\ T)^{1/2}\ ] > 0$.

As can be seen in the figure, we are now able to distinguish between the chaotic behaviour caused by close encounters with Mars (yellow full dots) and that caused by the overlapping of resonances or other criteria (red asterisks). A question that naturally arises is about the long-term stability of the chaotic objects that are Mars crossing. Are all these objects protected by deep close encounters with Mars by the Kozai mechanism proposed by Milani et al. (1989), or are some of these objects relatively young bodies only recently inserted in unstable regions? Answering this question involves long-term dynamical simulations, which are beyond the purpose of this paper. But this issue remains an interesting topic for future work.

The next logical step was obtaining estimates of Lyapunov times for regions where no current or few asteroids are found. This is especially important for example for the regions that were found to be stable in Section 8, but show a small density of asteroids. One may wonder if the small asteroid density may be caused by a long-term dynamical effect, or if it is primordial. One useful tool to obtain information on the long-term stability of orbits may be obtaining MLEs.

To estimate MLEs for orbits in the region, I used a modified version of SWIFT-LYAP2.F, a code that integrates the difference equation (Mikkola & Innanen 1999; Morbidelli 2002) in the SWIFT package (Levison & Duncan 1994). For each of the test particles, I integrated the difference equation with an initial difference vector of modulus $d(0) = \sqrt{6} \times 10^{-9}$, and determined the modulus $d(t)$ of the displacement vector between the two vectors at time t.

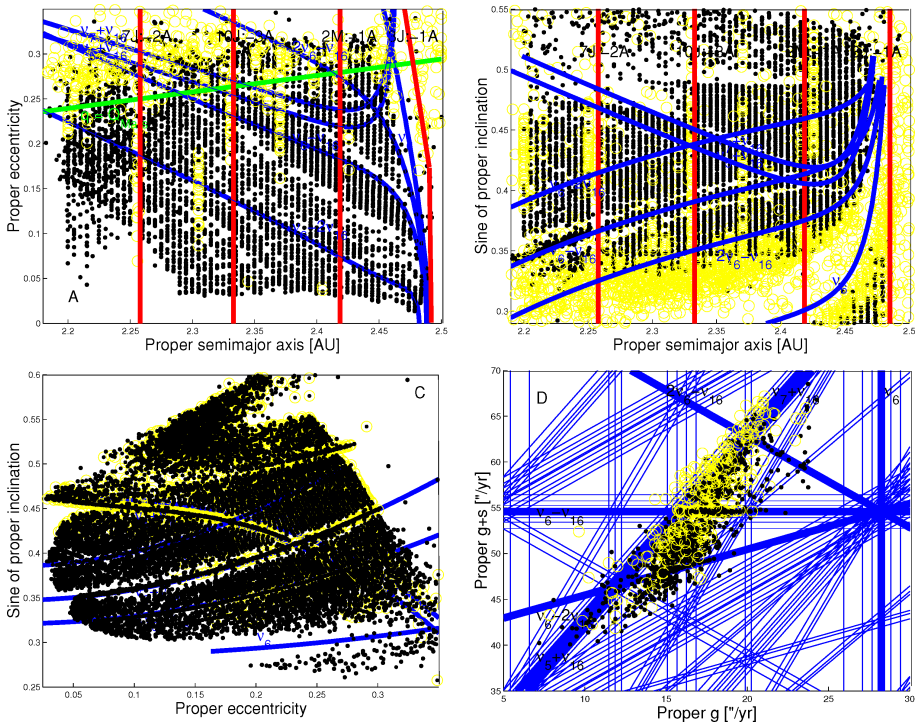

Figure 12. Lyapunov times projected in the space of averaged (a, e) (panel A), (a, sin(i)) (panel B) and (e, sin(i)) (panel C) elements. Panel D displays the Lyapunov times of real asteroids in the local background in the (g, $g - s$) space of proper frequencies. Yellow circles display Lyapunov times smaller than 20 000 yr, while black dots are associated with times larger than 20 000 yr.

I constructed a series (t, ln[$d(t)/d(0)$]), and performed a linear least-square fit on this series. Since $d(t) \simeq d(0)\exp(Lt)$, where L is the Lyapunov exponent, the slope of ln[$d(t)/d(0)$] versus time is equal to the maximum Lyapunov exponent. More information on the procedure used to obtain MLEs can be found in Carruba et al. (2004).

Fig. 12 displays a projection in the space of averaged elements of the Lyapunov times obtained for a 20 Myr numerical simulation. I used 5300 particles in the (a, e) plane, 9060 particles in the (a, sin(i)) plane, and 13 590 test particles in the (e, sin(i)) plane near the Phocaea family. I also used a step in a of 0.005 au, in e of 0.004 and in i of 0.°1, and took particles in an equally spaced grid of 60 by 90 particles in the (a, e) plane, of 60 by 151 particles in the (a, sin(i)) plane and of 90 by 151 particles in the (e, sin(i)) plane.[5] The initial values of sin(i), e, a (for the simulations in the (a, e)), (a, sin(i))- and (e, sin(i)) planes, respectively), and initial angular elements Ω, ω and λ of the test particles were fixed at those of (25) Phocaea at J2000.

In order to study the orbital evolution of asteroids in the region of the Phocaea families, I also performed an integration with the SWIFT-MVS integrator of Levison & Duncan (1994), modified by Mira Brož to include the second-order symplectic map from Laskar & Robutel (2001) (the code is publically available at http://sirrah.troja.mff.cuni.cz/mira/mp/) and the same test particles used for obtaining MLEs. All planets from Venus to Neptune were included in the simulation. Mercury was accounted for as a barycentric correction of the initial conditions. Non-singular orbital elements were Fourier filtered on line to eliminate all periods smaller than 600 yr, and averaged elements were obtained over the whole length of the integration.

[5] My test particles covered a range between 2.2 and 2.5 au in a, 0 and 0.36 in e and 15° and 30° in i, respectively.

Table 3. Argument and semimajor axis location of the main three-body resonances in the region of the Phocaea group.

Three-body resonance	Semimajor axis a (au)
9J:-5S:-2A	2.25838
3J:1S:-1A	2.30189
8J:-3S:-2A	2.30229
5J:-4S:-1A	2.30270
9J:-6S:-2A	2.34884
2J:3S:-1A	2.39647
4J:-2S:-1A	2.39736
6J:-7S:-1A	2.39825
7J:-2S:-2A	2.44847
9J:-7S:-2A	2.44893

The main two-body mean-motion resonances in the region (7J:-2A, 10J:-3A, 2M:-1A, 3J:-1A) are displayed in Fig. 12 (panels A and B). The limits of the 3J:-1A resonance in Fig. 12 (panel A) are defined according to equation (3) in Morbidelli & Vokrouhlický (2003). Table 3 reports the resonant argument and approximate location in the semimajor axis of the main three-body resonances, as identified by Michtchenko et al. (2009) (for simplicity, they are not shown in Fig. 12). The thick blue lines in Fig. 12 (panels A, B and C) display the location of the centre in the average element space of the main secular resonances in the region.

Yellow circles display Lyapunov times smaller than 20 000 yr, while black dots are associated with times larger than 20 000 yr. The green line in Fig. 12 (panel A) displays the location of orbits with $q = Q_{\rm Mars}$. As can be seen in Fig. 12 (panel A), most of the chaos is confined to the region of close encounters with Mars.

Vertical 'strips' of small Lyapunov times are associated with two-body mean-motion resonances or (not shown) three-body mean-motion resonances such as the 5J:-4S:-1A resonance. For what concerns the (a, sin(i)) projection (Fig. 12, panel B), I notice that there is a region of very low Lyapunov times in the proximity of the ν_6 secular resonance. In particular, almost no particle with inclination lower than that of the ($2\nu_6 - \nu_{16}$) resonance has Lyapunov times larger than 20 000. While the study of dynamical evolution of test particle on a time-scale longer than the 20 Myr used here for obtaining dynamical maps is beyond the purposes of this article, it is reasonable to expect that the chaotic region near the ν_6 resonance may reveal to be unstable on a time-scale of 100 Myr or more, in the same way as the analogous region near the 3J:-1A mean-motion resonance was found to be (Guillens, Vieira Martins & Gomes 2002). I believe that a more in-depth study of the chaotic layer found in this work, possibly caused by the overlapping of several non-linear secular resonances near the ν_6 resonance, may be an interesting topic for future research.

Fig. 12 (panel C) displays the results for the (e, sin(i)) plane. As can be seen in the figure, the zone of chaos associated with the Mars-crosser area for eccentricities larger than 0.22 is also found in this plane. The area of chaos near the ν_6 secular resonance is also encountered at low values of sin(i).

Finally, Fig. 12 (panel D) displays a projection of real asteroids in the Phocaea family local background in the (g, $g - s$) space. Chaotic bodies tend to be found beyond the ($2\nu_6 - \nu_{16}$) resonance, as also observed in the (a, sin(i)) survey. Other chaotic bodies are associated with Mars-crossing orbits (see Fig. 12, panel A).

9 CONCLUSIONS

In this work, I reviewed the current knowledge on the Phocaea dynamical family region. Among other things, I did the following.

(i) Obtained families and clumps in the domain of proper elements and frequencies (Carruba & Michtchenko 2007, 2009). With the exception of the family around (19536) (1999 JM4), formerly associated with the clump around (2860) Pasacentennium, the families and clumps found by Gil-Hutton (2006) are now substructures of the Phocaea family. Also, an interesting side result of this paper was the clump associated with (6246) Komurotoru. This, to my knowledge, is the first clump detected only in the frequency domain. It may be the first of a series of new 'frequencies' clumps and families that may be about to be discovered.

(ii) Revised the current knowledge on the taxonomy of objects in the Phocaea family region and found that most of the S-type objects in the region are members of the Phocaea families.

(iii) Obtained principal components based on the SDSS-MOC4 data, and used this information to obtain families in the space of colours and proper elements and colour and proper frequencies (Carruba & Michtchenko 2007, 2009).

(iv) Revised the current knowledge on absolute magnitudes and geometric albedos for objects in the region. Most of the objects with known albedo in the range between 0.10 and 0.25 (characteristic of S-type bodies) are members of the Phocaea families.

(v) Obtained Yarkovsky isolines and C-target function values (equation 6) for members of the Phocaea families. Using standard values for the Yarkovsky parameters for S-type objects, I obtained an upper limit for the age of the family of 2.2 Byr. Refining the family age estimate using the Monte Carlo approach of Vokrouhlický et al. (2006a,b,c) will be difficult, since the family age seems to be beyond the time-scales for which the YORP effect is correctly modelized. The family is also highly asymmetrical in the semimajor axis, and asteroids with a semimajor axis larger than that of the family barycentre seems to have been significantly depleted, possibly because of the effect of the local dynamics (see Section 8).

(vi) Computed the cumulative absolute magnitude H distribution ($N(<H)$) for the two Phocaea families. As in Parker et al. (2008), the Phocaea family distribution seems to be best approximated by a broken power law, for two intervals in H between 12 and 14 and between 14 and 15. While values of the γ exponents that fit the first interval are compatible with typical values found for inner main belt families, the values for the second interval are significantly lower, possibly suggesting a dynamical erosion for smaller sized objects.

(vii) Obtained the values of intrinsic collision probabilities for members of the Phocaea family with (25) Phocaea itself, (8) Flora and (15) Eunomia. The average collision probability of colliding with (8) Flora, a low-inclination inner main belt body, was even larger than that of impacting (25) Phocaea, suggesting that collision with inner main belt objects may have played an important role in the history of the Phocaea family.

(viii) Studied the available information on rotation rates for asteroids in the Phocaea family groups (Warner et al. 2008). 18 bodies have estimates for their rotation periods, and a histogram of the rotation frequencies shows that there is an excess of slow rotators, explainable in the framework of evolution of the spin axis via the YORP effect.

(ix) Obtained dynamical maps of averaged elements for grids in (a, e), (a, sin(i)) and (e, sin(i)) of osculating initial conditions and identified the mean-motion and secular resonances that seem to have a larger effect on the short-term (20 Myr) stability of asteroid averaged elements. The Phocaea family is bounded by a region delimited by the 7J:-2A mean-motion resonance at low a, the 3J:-1A mean-motion resonance at high a, the ν_6 secular resonance at low i and a region of close encounters with Mars at high e. It is characterized by its interaction with the ($\nu_6 - \nu_{16}$) secular resonance (Carruba & Michtchenko 2009). A stable region of a low asteroid density between the ($2\nu_6 - \nu_{16}$) and the ν_6 resonances in the (a, sin(i)) plane was identified, and further studied via the use of chaos indicators.

(x) Revised the values of MLE available in the literature for asteroids in the Phocaea family region and obtained MLEs for the same grids of initial conditions used to obtained averaged element maps. Areas of low Lyapunov time $T_L < 20\,000$ are associated with (i) two- and three-body mean-motion resonances, (ii) a zone of encounters with Mars and (iii) a region near the ν_6 separatrix, associated with the stable region of low-density asteroids identified with the averaged elements maps.

At the end of this preliminary analysis of the Phocaea family region there is a general vision of the origin and evolution of asteroids in the region that is starting taking shape. While it is certain that the Phocaea group is indeed in a stable island surrounded by very unstable dynamical regions (Knežević & Milani 2003), the fact that most of the S-type objects are associated with the dynamical Phocaea families seems to suggest that the Phocaea cluster should indeed be a real collisional family. No local background was identified in the cumulative H distribution, and it seems that the region, apart from a few large C-type objects, is dominated by the Phocaea family. This may suggest that very few bodies reached the highly inclined region studied here and, of those, one, the parent body of the Phocaea family, was targeted in the collision that created the family possibly up to 2.2 Byr ago. Values of collision probabilities suggest that the impactor may have come from the low i inner main

belt, but of course the exact orbital location of the impactor may never been proved.

The family subsequently lost several of its members, especially at values of a larger than that of the family barycentre, due to the interaction with the local web of mean-motion and secular resonances. Only the part of the family having low C-target function values may have survived in this scheme.

More important than the question that this work may have answered are, in my opinion, the new questions that arise from this paper. One of these questions regards the long-term stability of the smaller families and clump identified in this work in both proper element and frequency domains. How stable in time are the smaller families and clumps other than the Phocaea family, if we investigate the evolution of orbital elements caused by the Yarkovsky effect? Are these groups statistically significant and really associated with break-up of parent objects, or are they just a random association of objects that do not share a common origin? This in my opinion is particularly important for what concern the new frequency cluster around (6246) Komurotoru.

Another important question regards the objects that are present in the region and should not be there, i.e. the chaotic Mars crossers at $e > 0.3$. Knežević & Milani (2003) observed that these objects may be in the Kozai class of planetary close encounters, and that therefore could be protected by experiencing very close encounters with Mars. They therefore suggested that this population of objects might be primordial. Understanding the long-term evolution and stability of this kind of orbits, especially when the Yarkovsky effect is also considered, is a task that, however, to my knowledge, has not yet been performed.

Finally, on what time-scales, if any, are orbits in the chaotic region near the ν_6 separatrix unstable? What resonance overlapping is exactly causing the chaotic dynamic in the region? Many of these new questions may be answered only performing simulations on time-scales much longer than the 20 Myr used to obtain dynamical maps in this work. Answering these questions seems therefore to exceed the purpose of this paper, which was starting exploring the current state of the knowledge on the Phocaea family region. But they are certainly very interesting possible projects for further research, worth exploring in future works.

ACKNOWLEDGMENTS

I am grateful to the reviewer of this article, David Vokrouhlický, for helpful comments and remarks that helped us to improve this work. I would like to thank the São Paulo State Science Foundation (FAPESP) that supported this work via the grant 06/50005-5 and the Brazilian National Research Council (CNPq). I am also grateful to the Physics and Astronomy department of the IPD/UNIVAP for the use of their facilities.

REFERENCES

Beaugé C., Roig F., 2001, Icarus, 153, 391
Bendjoya P., Zappalà V., 2002. Asteroids III, Univ. of Arizona Press, Tucson, p. 613
Benettin G., Galgani L., Giorgilli A., Strelcyn J. M., 1980, Meccanica, 15, 9
Bottke W. F., Durda D. D., Nesvorný D., Jedicke R., Morbidelli A., Vokrouhlický D., Levison H., 2005, Icarus, 175, 111
Brož M., Vokrouhlický D., 2008, MNRAS, 390, 715
Bus J. S., Binzel R. P., 2002a, Icarus, 158, 106
Bus J. S., Binzel R. P., 2002b, Icarus, 158, 146
Carruba V., 2009, MNRAS, 395, 358
Carruba V., Michtchenko T., 2007, A&A, 475, 1145
Carruba V., Michtchenko T., 2009, A&A, 493, 267
Carruba V., Burns J., A., Bottke W., Nesvorny D., 2003, Icarus, 162, 308
Carruba V., Nesvorný D., Burns J. A., Ćuk M., Tsiganis K., 2004, AJ, 128, 1899
Carvano J. M., Lazzaro D., Mothé-Diniz T., Angeli C., 2001, Icarus, 149, 173
Farinella P., Vokrouhlický D., Hartmann W. K., 1998, Icarus, 132, 378
Foglia S., Masi G., 2004, Minor Planet Bull., 31, 100
Fukugita M., Ichikawa T., Gunn J. E., Doi M., Shimasaku K., Schneider D. P., 1996, AJ, 111, 1748
Greenberg R., 1982, AJ, 87, 184
Guillens S. A., Vieira Martins R., Gomes R. S., 2002, AJ, 124, 2322
Gil-Hutton R., 2006, Icarus, 183, 93
Knežević Z., Milani A., 2003, A&A, 403, 1165
Laskar J., Robutel P., 2001, Celest. Mech. Dyn. Astron., 80, 39
Lazzaro D., Angeli C. A., Carvano J. M., Mothé-Diniz T., Duffard R., Florczak M., 2004, Icarus, 172, 179
Levison H., Duncan M. J., 1994, Icarus, 108, 18
Lyapunov A. M., 1907, Ann. Fac. Sci. Univ. Toulose, 9, 203
Migliorini F., Zappalà V., Vio R., Cellino A., 1995, Icarus, 118, 271
Mikkola S., Innanen K. A., 1999, Celest. Mech. Dyn. Astron., 74, 59
Milani A., Knežević Z., 1994, Icarus, 107, 219
Milani A., Carpino M., Hahn G., Nobili A., 1989, Icarus, 78, 212
Morbidelli A., 2002, Modern Celestial Mechanics: Dynamics in the Solar System. Taylor & Francis, London
Morbidelli A., Vokrouhlický D., 2003, Icarus, 163, 120
Nesvorný D., Jedicke R., Whiteley R. J., Ivezić Ž. 2005, Icarus, 173, 132
Parker A., Ivezić, Ž., Jurić M., Lupton R., Sekora M. D., Kowalski A., 2008, Icarus, 198, 138
Pravec P. et al., 2008, Icarus, 197, 497
Roig F., Gil-Hutton R., 2006, Icarus, 183, 411
Tedesco E. F., Noah P. V., Noah M., Price S. D., 2002, AJ, 123, 1056
Tholen D. J., 1989, in Binzel R. P., Gehrels T., Matthews, M. S.. eds, Asteroid Taxonomic Classifications. University of Arizona Press, Tucson, p. 298
Vokrouhlický D., 1998, A&A, 375, 1093
Vokrouhlický D., Brož M., Morbidelli A., Bottke W. F., Nesvorný, Lazzaro D., Rivkin A. S., 2006a, Icarus, 182, 92
Vokrouhlický D., Brož M., Bottke W. F., Nesvorný D., Morbidelli A., 2006b, Icarus, 182, 118
Vokrouhlický D., Brož M., Bottke W. F., Nesvorný D., Morbidelli A., 2006c, Icarus, 183, 349
Warner B. D., Harris A. W., Pravec P., 2008, Asteroid Lightcurve Data Base (LCDB), http://www.MinorPlanetObserver.com
Warner B. D., Harris A. W., Vokrouhlický D., Nesvorný D., Bottke W. F., 2009, Icarus, submitted
Xu S., Binzel R. P., Burbine T. H., Bus S. J., 1995, Icarus, 115, 1
Zappalà V., Cellino A., Farinella P., Knežević Z., 1990, AJ, 100, 2030
Zappalà V., Bendjoya P., Cellino A., Farinella P., Froeschlé C., 1995, Icarus, 116, 291
Zellner B., Tholen D. J., Tedesco E. F., 1985, Icarus, 61, 355

This paper has been typeset from a TEX/LATEX file prepared by the author.